Chemical characterisation of variably degraded fibre glass reinforced plastic from the marine environment

Laurence Hopkinson*, Stanislav Ostapishin, Petra Kristova, Katy Hamilton, Corina Ciocan

*Corresponding author

e.mail addresses: l.hopkinson@brighton.ac.uk; S.Ostapishin1@uni.brighton.ac.uk;

P.Kristova@brighton.ac.uk: K.Hamilton5@uni.brighton.ac.uk; C.Ciocan@brighton.ac.uk

University of Brighton, School of Applied Science, Brighton BN2 4GJ, United Kingdom

Key words: fibre glass reinforced plastic, mid infrared, E-glass, poly diallyl phthalate, polyester

Abstract

Glass reinforced plastic (GRP) constitutes the commonest component of small sea going craft of all descriptions. This study provides a baseline molecular and elemental account of GRP's recovered from the marine environment. Fourteen samples of GRP sourced from scrapyards and one sample sourced from a GRP boat manufacturer were examined. Samples were analysed by x-ray fluorescence and mid infrared (MIR). The latter technique confirmed that all samples contained the same polyester resin, poly diallyl phthalate (PDP). The two techniques in combination indicate the presence of aluminium calcium borosilicate E-glass fibres (E denotes electrical) of variable origins. MIR results are consistent with hydrolysis of polyester, weakening of the glass fibre resin interface facilitating exposure of e-type fibres to water which accelerates fibre breakage. The implication being that aging of GRP in the marine environment represent sources for micro (<5mm) and macro plastic release, plus fragmented asbestiform-like silicate fibres.

Globally, fibre glass reinforced plastic also known as glass reinforced plastic (GRP) is a firmly established durable and integral component of small sea going crafts of all descriptions and, has been widely employed in boat fabrication since the middle of the 20th century. A growing number of end-of-life vessels end up in landfill or abandoned in estuaries (e.g. Rees et al., 2014, Turner et al., 2016; Bray 2019). Environmental degradation can result in GRP breaking down into its component parts, in the form of plastics and fibre glass. In addition, microparticles can be released when the boats are crushed, dismantled or just repaired (Bray 2019). The durability of GRP's is determined by that of the component parts: glass fibres, matrix resin, and the interface between them (Schutte 1994).

GRP is a composite consisting of glass fibres arranged in a variety of weave patterns fixed in a thermoset resin. The most common glass type employed in GRP production is E-glass (where E denotes electrical), which is characteristically employed where strength and high electrical resistivity are required (Hartman et al., 1996). The composition of E-glass is commonly given as weight per cent oxides (wt%) *ca*: CaO 16 %; Al_2O_3 14.5 %; B_2O_3 9.5 %; MgO 5%; Na_2O and K_2O 1%; SiO_2 55% (Bascom 1974; Schutte 1994). However, chemical variation in glass types occurs, as a consequence of raw materials, and/or different environmental constraints at manufacturing sites (Hartman et al., 1996). Compositional fluctuations within a glass type are not believed to significantly alter the physical or chemical properties of the glass (Hartman et al., 1996). However, fiberglass does have similar chemical and physical properties to asbestos, i.e. minerals which can be separated into thin, long fibres composed of Si and O in association with other inorganic materials (Galimany et al, 2009).

Environmental attack degrades GRP chemically and physically overtime with exposure to moisture. The resin may plasticize, swell, or microcrack, in addition to potential degradation of the fibre matrix by either chemical and or mechanical attack (Schutte 1994). The physically weakest portion of the composite is generally considered to be the fibre-matrix interface (Ishida and Koenig 1978). Consequently, silane treatment of glass fibre surfaces is commonly undertaken to improve the wet strength of GRP's (e.g., Ishidi and Koenig 1978). Polyesters are widely employed as the thermoset resin. A recurring mechanism of polyester aging is attack by humidity, i.e. hydrolyses (Hunter et al., 2000). The environmental impact of physically and chemically degraded GRP on the marine environment is uncertain although GRP degradation seems certain to contribute to microplastic (<5mm) production within the natural environment. Further, laboratory studies indicate that detrimental effects to organisms with respect to swimming impairment and fibreglass ingestion as a result of exposure to powdered GRP in aqueous solutions (Ciocan et al., 2020).

This study delivers the first molecular spectroscopic examination of GRP in conjunction with elemental characterization of GRP's which have been variably weathered and degraded within the marine environment. The fourteen samples were sourced from defunct GRP fabricated boat wrecks at breakers yards within the South coast of England (U.K); together with a sample of unused GRP supplied by a South coast boat manufacturer (sample UU).

Photographs of the samples are presented in Figure 1. From visual inspection it is evident that the GRP surfaces vary in terms of colour, brightness, and in terms of reflectivity of light, from a gloss transparent resin finish through to a matt finish, in descending order of gloss finish: 13, 11, 12, UU,4, 2, 10, 1, 3, 5, 14, 8, 6, 7, 9. Changes in brightness of samples have previously been interpreted in terms of debonding or cracking of resin matrices (Morii et al., 1993). It is also evident that samples vary in the extent to which fibres show surface relief relative to the enclosing resin and that, in places, friable strands of fibre glass project through GRP surfaces. In common with commercial asbestos, fibres within all GRP's examined display aspect ratios (length/ width) of greater than 20:1, although aspect ratio alone cannot be used as the only criterion for asbestos identification (Wylie 1979). It is also evident that outer surfaces include variably degraded paints.

A (X-Met) portable energy dispersive x-ray fluorescence (PXRF) analyser was employed in order to characterise major and trace elemental abundances within the GRP from the fifteen fragmented boat samples. The device employs a standard 9mm aperture and the tube is 45Kv with a Rh target. Acquisition time is 90 seconds. The device was calibrated against silicate soils matrices. Mid-infrared measurements were performed using a Perkin Elmer, Spectrum 65 spectrometer, fitted with an attenuated total reflectance (ATR) accessory employing a ZnSe crystal. Paint-free samples of GRP were powdered using an agate mortar and measured in the spectral range 4000-550 cm^{-1} at a resolution of 4 cm^{-1}. Measurements through the ATR accessory requires firm contact between the sample and the ZnSe crystal. This was achieved by uniform light manual compaction. Each spectrum was collected from 16 scans and repeated on different subsamples to assure representative spectral information. All analyses were conducted at 25 °C, at atmospheric pressure at the University of Brighton U. K.

Table 1 shows the PXRF analyses for the fifteen samples. The analyses were conducted where possible in areas where the fibres were exposed and no visibly discernible paint was in the path of the X-Ray beam. This was not always possible, where paint was incorporated in the analysed area elevated levels of TiO_2 and or Fe_2O_3 were recorded alongside elevated traces of Co (Table 1). Pb, Cu and Zn have

previously been identified as heavy metals of concern in degraded marine craft paints (Rees et al., 2014). In the samples presented here the highest concentrations of Cu and Zn coincide with the highest Fe_2O_3 content suggesting that the two trace elements are paint associated. Sample 2 shows an anomalously high Pb concentration which also coincides with a high Fe_2O_3 content (Table 1). It has previously been documented that the abundance of Pb in older paints is of particular environmental concern (Rees et al., 2014).

All samples show enrichment in SiO_2 and CaO with subordinate Al_2O_3, and consistently less than 2 wt% K_2O. The oxides Al_2O_3, SiO_2 and CaO were normalized to give insight into the proportionality variability in relation to a range of commercial high strength glass fibres employed in reinforced glass composites (Figure 2) as reported by Hartman et al. (1996). The fifteen samples are most compositionally similar to E glass and ECRGLAS®. It should be noted that many of the fifteen samples are variably depressed in SiO_2 content relative to published values of the commercial E-type glasses. Possible reasons are multiple, e.g., manufacturer specific variability in the concentration of boron (which cannot be detected by the PXRF) employed at the expense of SiO_2. In addition, aqueous solutions can leach alkalis and alkaline-earth metals as well as CaO, MgO, Al_2O_3 and B_2O_3 from E-glass (Schutte 1994). Hence, the fifteen sampled boats are interpreted as containing E-type glasses of varied origins and manufacture.

All MIR spectra show a search score of 0.81 or greater in profile match with poly diallyl phthalate (PDP) when compared against the Perkin Elmer, polymer library. The sample UU matched with a score 0.86 and shows visually overlap with library standard. However, UU sample has significantly lower spectral intensity in comparison to library spectrum possibly due to loading with glass fibres. Assignments for prominent PDP related bands in the MIR spectra are given in Figure 3. Close inspection of the MIR strong carbonyl band at 1720cm^{-1} indicates the presence of a subtle shoulder at *ca* 1740cm^{-1} in all spectra, consistent with the presence of esters.

The MIR spectra show a range of generally broad low to moderate intensity bands which cannot be assigned specifically to PDP. In particular the PDP assigned band at 1064cm^{-1} (ascribed to deformation of aromatic rings) shows a prominent shoulder at 1040cm^{-1}. Variably resolved weak overlapping bands are also evident at *ca* 920 and 847cm^{-1}. In addition, the well resolved PDP related band at 742cm^{-1} shows a poorly resolved shoulder at *ca* 764cm^{-1} (Figure 3).

Silicate glasses lack the long-range order observed in crystals, hence they have broad and smooth infrared and Raman spectral features (Wang et al., 2016). Bands in the 1000-1200cm^{-1} region are consistent with [Si-O-Si] asymmetric stretches associated with silicate glasses, those in the 600 to 850cm^{-1} region are generally assigned to [Si-O-Si] symmetric stretches (Efimov 1996). At longer wavenumbers (> *ca* 2450cm^{-1}) the spectra show additional bands assigned to the resin, superimposed on a broad low intensity feature at *ca* 2450-3600cm^{-1} assigned to the water related envelope (e.g., Efimov et al., 2003). Two spectra also show a low intensity sharp band at 3690cm^{-1} which could be assigned to free [Si-OH].

The MIR spectra show a variably resolved band at *ca* 1040cm^{-1} which closely coincides with a band reported at 1038cm^{-1} from E-type glass (Ishida and Koenig 1980) and is assigned to the [Si-O-Si] asymmetric stretch (Figure 3). Figure 4 shows the absorption intensity at 1040cm^{-1} divided by background absorption at 4000cm^{-1} (1040cm^{-1}/4000cm^{-1}) and the 1720cm^{-1} band (assigned to the resin-related carbonyl stretch) divided by background absorption at 4000cm^{-1} (1720cm^{-1}/4000cm^{-1}). A reasonable correlation is suggested (r^2= 0.834), consistent with sample 9 containing the highest concentration of E-type glass and carbonyl relative to all samples. Sample [UU] shows the lowest (1040cm^{-1}/4000cm^{-1}) absorption intensity ratio. Visible inspection of 9 indicates that the sample is highly physically degraded. Hence data is consistent with fibre exposure during GRP degradation. Sample [9] also shows the highest (1720cm^{-1}/4000cm^{-1}) absorption intensity ratio. This result appears significant because hydrolysis of polyester results in disentanglement of long molecular chains when ester links are cleaved by chemical reaction with water, yielding a carbonyl group and an alcohol group, culminating in a loss of polyester hardness with disentanglement of long molecular chains (Hunter et al., 2000). Hence MIR data is consistent with the detection of chemical degradation of polyester accompanying progressive silicate fibre exposure.

Poorly resolved weak bands at 920cm^{-1} and 847cm^{-1} are evident in all MIR spectra. These bands cannot be readily assigned to PDP. However, the origin(s) of these bands remain uncertain because of the strong overlap between bands associated with the bulk fibre (Si-O-Si) and (Si-OH) associated with silane coupling agents (Ishida and Koenig 1978). The inorganic part of which yields an extremely strong absorbance (Ishida and Koenig 1980). The two bands reported here at 920cm^{-1} and 847cm^{-1} closely coincide with bands reported at 920cm^{-1} and 840cm^{-1} which have been assigned to [Si-OH] modes associated with silane additives on E-glass fibres (Ishida and Koenig 1980) and, consequently are similarly assigned here. The same experimental study showed that variability in the concentration of

silane treating solutions employed during fibre preparation occurs and, that the amount of the silane on E-glass fibres decreases with exposure in water (Ishida and Koenig 1980).

Figure 5 shows the absorption intensity ratio of the band at 920cm^{-1} ratioed against the 1040cm^{-1} [Si-O-Si] antisymmetric stretching mode (1040cm^{-1}/920cm^{-1}) plotted against the (1040cm^{-1}/4000cm^{-1}) absorption intensity ratio. The fifteen samples display a reasonable potential linear correlation (r^2 = 0.654). Of note sample 9 shows the highest (1040cm^{-1}/920cm^{-1}) absorption intensity ratio. Hence, even if the trend is not linear, data is suggestive of high adsorption intensity ratio relating to degradation. Given the physically degraded nature of sample 9 and evidence for chemical degradation of polyester in the same sample, the data is consistent with not only separation of resin from fibres during environmental degradation but also loss of silane additive from the fibres themselves. With further work we may be able to determine linearity or a cut off at which degradation accelerates. All E-glasses contain metal oxides meaning they are intrinsically alkaline and hygroscopic, thus loss of resin and fibre coatings combined with exposure to water facilitates stress corrosion of the fibres and failure (Schmitz and Metcalfe 1966).

Polyesters can undergo hydrolytic main chain scission to form water and soluble fragments, nevertheless the hydrolysis of polyesters under neutral conditions is slow (Pickett and Coyle, 2013). In general, the changes to polymer and loss of molecular weight has a dramatic effect on the service life and mechanical properties even if only one to two percent of the ester units are hydrolysed (Pickett and Coyle, 2013). Therefore, these changes linked to resin hydrolysis may be too subtle to be observed in MIR spectrum of PDP as no increase or presence of OH groups (e.g. in area 3300cm^{-1}) were detected during our investigation. Sample UU showed very weak broad peak in area below 3700cm^{-1} similarly found in all degraded samples. However, we observed effects of possibly hydrolytic erosion and changes in ratio of resin to glass content and within glass fibres.

XRF and MIR analysis appear to give insight into the chemical variability in GRP inherent from the various site-specific manufacturing processes. Previous research has shown that many factors contribute to the failure of GRP's on exposure to the environment (Schutte 1994). The dominant mode of failure can be due to failure of the matrix, glass fibres, the matrix-glass interface, or any combination thereof (Schutte 1994). In this respect MIR analysis of the GRP's appears to offer insight into the chemical pathway of GRP degradation through ester links being cleaved by chemical reaction with water and loss of silane fibre coatings, with resultant embrittlement of glass fibres (Schutte 1994). Amongst all plastics released into the marine environment polyester is the dominant pollutant, with

polyester microfibres from clothing and textiles being singled out as of being of particular concern (Mishra 2019; Fontana et al., 2020). Evidence presented here suggests that marine craft are additional sources for the release of polyester in the form of a significant range of particle sizes, alongside fragmented alkaline hygroscopic silicate fibres with aspect ratios comparable to commercial asbestos; plus, fragments of heavy metal bearing paints of varied chemistries. In conclusion, several known highly hazardous pollutants were found in GRP pieces associated with old/new boat hulls and they have the capacity to severely impact both the wildlife and human health. Leachates from old/abandoned boats were shown to be toxic to organisms of several trophic orders and our results herein underline that boat maintenance facilities, and scrapyards in general, should be better regulated to minimize further exposure and spread of contaminants in the environment. Looking forward, monitoring the state of degradation using techniques such as described in this baseline study will be important for estimating further breakdown.

Acknowledgements

This research was funded by the University of Brighton.

References

Bascom W.D (1974) The surface chemistry of moisture-induced composite failure, in E.P. Plueddemann (ed.), Interfaces in Polymer Matrix Composites, Academic Press, New York, pp. 79-108.

Bray S (2019) End-of-Life Management of Fibre Reinforced Plastic Vessels: Alternatives to at Sea Disposal. International Maritime Organisation, CPY Group UK. https://wwwcdn.imo.org/localresources/en/OurWork/Environment/Documents/Fibre%20Reinforced%20Plastics%20final%20report.pdf

Ciocan C, Kristova P, Annels C, Derjean M, Hopkinson L, (2020) Glass reinforced plastic (GRP) a new emerging contaminant - First evidence of GRP impact on aquatic organisms, Marine Pollution Bulletin 160, 1-8.

Efimov A.M (1996) Quantitative IR spectroscopy: Applications to studying glass structure and properties. Journal of Non-Crystalline Solids. 203, 1-11.

Efimov A.M, Pogareva V.G, Shashkin A.V (2003) Water-related bands in the IR absorption spectra of silicate glasses. Journal of Non-Crystalline Solids 332, 93-114.

Fontana G.D, Mossotti R, Montarsolo A (2020) Assessment of microplastic release from polyester fabrics: the impact of different washing conditions. Environmental Pollution, 264, 1-6. https://doi.org/10.1016/j.envpol.2020.113960

Galimany E, Ramón M, Delgado M (2009) First evidence of fiberglass ingestion by a marine invertebrate (Mytilus galloprovincialis L.) in a NW Mediterranean estuary. Marine Pollution Bulletin 58(9):1334-8. DOI:10.1016/j.marpolbul.2009.04.027

Hartman D, Greenwood M.E, Miller D.M (1996) High strength glass fibres. AGY Technical paper. 1-12. https://www.agy.com/wp-content/uploads/2014/03/High_Strength_Glass_Fibers-Technical.pdf

Hunter L.W, White J.W, Cohen P.H, Biermann P.J (2000) A materials aging problem in theory and practice. John Hopkins APL Technical digest, 21, 575-581.

Ishidi H, Koenig J.L (1978) Fourier transform infrared spectroscopic study of the structure of silane coupling agent on E glass fiber. J Colloidal Interface Sci. 64, 565-576.

Ishida H, Koenig J.L (1980) Effect of Hydrolysis and Drying on the Siloxane Bonds of a Silane Coupling Agent Deposited on E-Glass Fibers. Journal of Polymer Science. Vol. 18, 233-237.

Mishra S, Rath C.C, Das A.K (2019) Marine microfiber pollution: A review on present status and future challenges. Marine Pollution Bulletin. 140, 188-197.

Morii T, Tanimoto T, Hamada H, Maekawa Z, Hirano T, Kiyosume K (1993) Weight changes of a randomly oriented GRP panel in hot water. Composites Science and Technology. 49, 209-216.

Pickett J.E, Coyle D.J (2013) Polymer Degradation and Stability, Vol. 98, Isssue 7, Pages 1311-1320.

Rees A, Turner A, Comber S (2014) Metal contamination of sediment by paint peeling from abandoned boats, with particular reference to lead. Science of The Total Environment, 494, 313-319.

Schmitz G.K, Metcalfe A.G (1966) Stress corrosion of E-glass fibers. Ind. Eng. Chem. Prod. Res. Dev. 5,1, 1-8.

Schutte C.L. (1994) Environmental durability of glass-fibre composites. Material Science and Engineering, R13, 265-324.

Turner, A., Rees, A., 2016. The environmental impacts and health hazards of abandoned boats in estuaries. Reg Stud Mar Science 6, 72–75. https://doi.org/10.1016/j.rsma. 2016.03.013.

Wylie A (1979) Fibre length and aspect ratio of some selected asbestos samples. Health Hazards of Asbestos Exposure. 330, 605-610. https://doi.org/10.1111/j.1749-6632.1979.tb18766.x

Table and Figure captions

Table 1. PXRF analyses of major (wt% oxides) and select trace elements. Note that n.d denotes not detected. Also, Ni and As are not presented in table 1 because both elements registered n.d. for all fifteen samples.

Figure 1. Photographs of GRP samples examined in this study, the two centimetre scale bar is provided for each photograph.

Figure 2. SiO_2, CaO and Al_2O_3 normalised values for a suite of commercial fibre glasses and the fifteen samples analysed in this study. Open circles indicate GRP types examined in this study. Solid red circles represent a range of commercial high strength glass fibres as reported by Hartman et al., (1996), where [A] denotes soda lime silicate glass. [AR] Alkali resistant glass composed of alkali zirconium silicates. [C] Calcium borosilicate glass, [D] Borosilicate glass. [E] Aluminium calcium borosilicate glass. [ECR] calcium aluminosilicate glass with maximum 2wt% alkalis. [R] Calcium aluminosilicate glass. [S2] Magnesium aluminosilicate glass.

Figure 3. Mid infrared spectra of GRP samples and assignments of peak bands. The inset diagram shows the peak fit resolved band at 1740cm^{-1} assigned to esters, which occurs as a shoulder on the prominent 1720cm^{-1} carbonyl band.

Figure 4. Absorption intensity at 1040cm^{-1} (assigned to the [Si-O-Si] asymmetric stretch) divided by background absorption at 4000cm^{-1} (1040cm^{-1}/4000cm^{-1}) and the 1720cm^{-1} band (assigned to the resin-related carbonyl stretch) divided by background absorption at 4000cm^{-1} (1720cm^{-1}/4000cm^{-1}).

Figure 5. Absorption intensity at 1040cm^{-1} (assigned to the [Si-O-Si] asymmetric stretch) divided by background absorption at 4000cm^{-1} (1040cm^{-1}/4000cm^{-1}), plotted against the (1040cm^{-1}/920cm^{-1}) absorption intensity ratio, the band at 920cm^{-1} is assigned to [Si-OH] modes associated with silane additives.

	Oxides weight percent							Elements parts per million			
Sample	SiO_2	Al_2O_3	CaO	K_2O	TiO_2	MnO	Fe_2O_3	Cu	Zn	Co	Pb
1	36.08	10.42	42.33	1.78	0.31	n.d	2.24	198	82	2063	219
2	36.05	9.66	34.91	0.73	7.76	n.d	4.64	257	n.d	2798	10377
3	42.53	13.54	36.09	1.16	0.18	n.d	1.21	147	75	1344	1318
4	28.00	9.69	28.30	0.71	28.94	n.d	1.31	n.d	82	1062	n.d
5	44.74	15.66	29.97	1.33	1.32	0.02	1.08	n.d	82	1161	95
6	41.28	6.02	23.52	n.d	18.60	0.35	2.29	596	751	4176	n.d
7	44.27	9.54	32.01	n.d	8.13	0.33	1.84	367	490	1652	n.d
8	30.55	9.40	33.28	0.81	21.28	0.04	1.25	227	82	452	n.d
9	45.58	13.62	25.77	0.95	0.43	0.10	11.81	1591	1577	n.d	621
10	47.60	13.35	32.94	1.18	0.36	n.d	2.04	272	368	933	n.d
11	37.34	9.26	40.40	1.50	2.12	n.d	1.97	187	141	4370	n.d
12	45.76	12.76	38.15	0.67	0.19	n.d	0.78	0	107	798	n.d
13	46.75	14.22	35.83	n.d	0.66	0.02	0.78	476	172	146	481
14	49.42	11.88	31.24	1.30	1.99	n.d	1.76	126	170	559	117
UU	34.42	8.74	48.2	n.d	1.25	n.d	2.08	426	n.d	4195	n.d

306

307

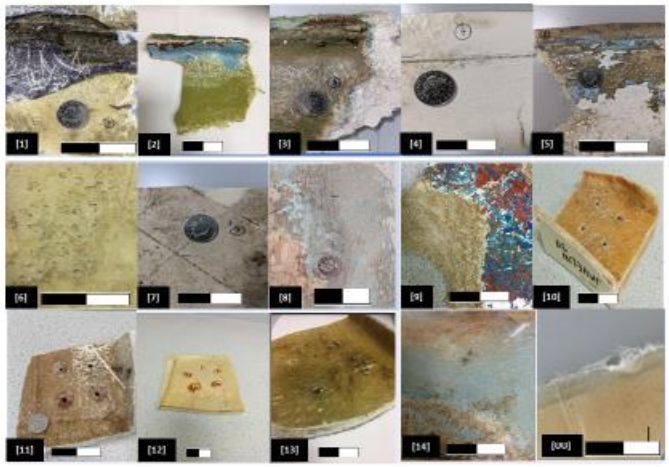

308

309

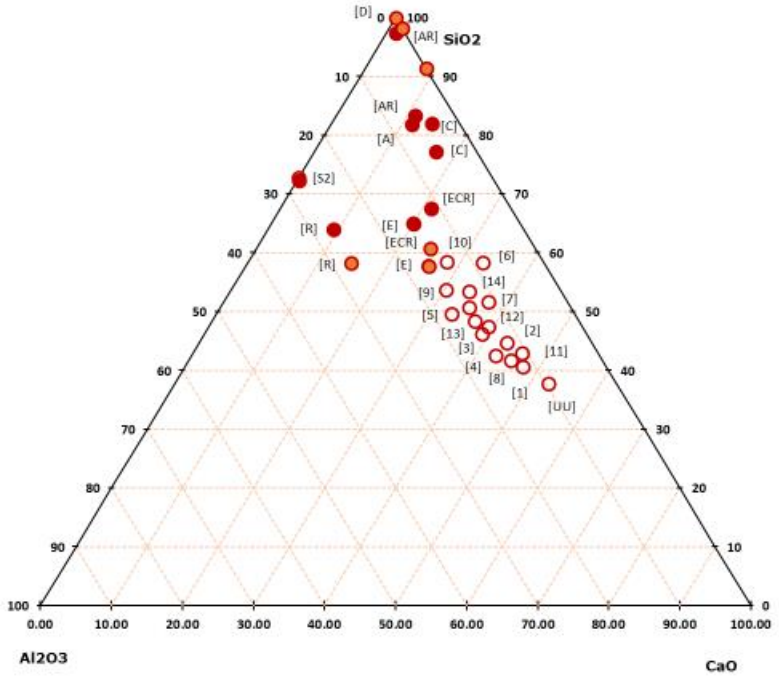
SiO2
Al2O3
CaO
[D]
[AR]
[A]
[C]
[S2]
[ECR]
[R]
[E]
[10]
[6]
[14]
[9]
[7]
[5]
[12]
[13]
[2]
[3]
[11]
[4]
[8]
[1]
[UU]
0.00
10.00
20.00
30.00
40.00
50.00
60.00
70.00
80.00
90.00
100.00

310

311

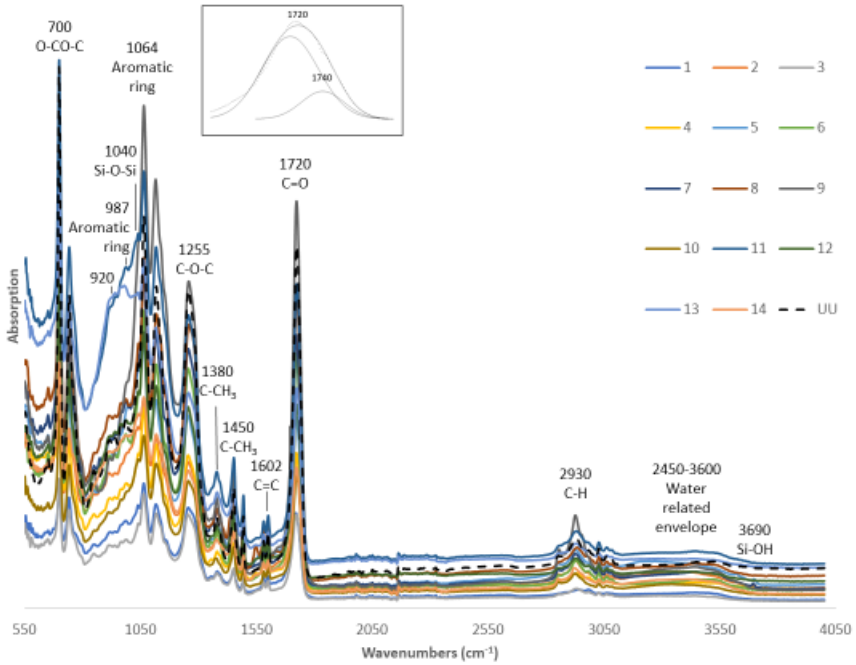
700
O-CO-C
1064
Aromatic
ring
1040
Si-O-Si
987
Aromatic
ring
920
1255
C-O-C
1720
C=O
1380
C-CH3
1450
C-CH3
1602
C=C
2930
C-H
2450-3600
Water
related
envelope
3690
Si-OH
1720
1740
1
2
3
4
5
6
7
8
9
10
11
12
13
14
UU
Absorption
550
1050
1550
2050
2550
3050
3550
4050
Wavenumbers (cm-1)

312

313

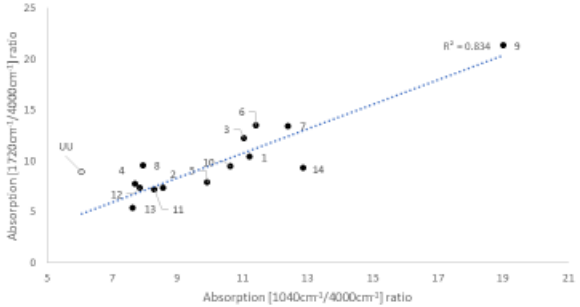
Absorption [1720cm⁻¹/4000cm⁻¹] ratio
Absorption [1040cm⁻¹/4000cm⁻¹] ratio
R² = 0.834
UU
0
9
6
3
7
1
8
10
4
2
5
14
12
13
11
25
20
15
10
5
0
5
7
9
11
13
15
17
19
21

314

315

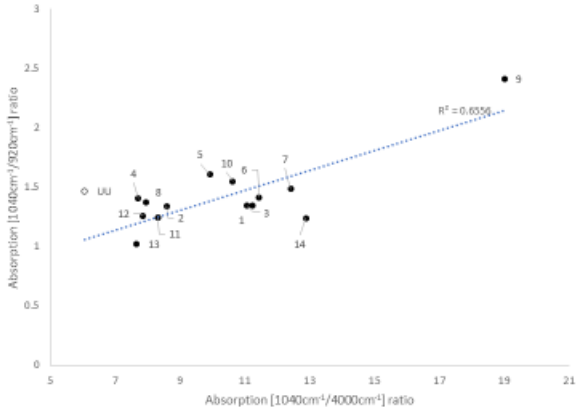
Absorption [1040cm-1/3280cm-1] ratio
Absorption [1040cm-1/4000cm-1] ratio
R² = 0.6556
UU
1
2
3
4
5
6
7
8
9
10
11
12
13
14

316